Supplementary Information

Ultrafine AuPd Nanoclusters on Layered Double Hydroxides by the Capt-Capped AuPd Cluster Precursor Method: Synergistic Effect for Highly Efficient Aerobic Oxidation of Alcohols

Jin Li, Yang Xu, Shuai Wang, and Hui Zhang *

State Key Laboratory of Chemical Resource Engineering, Beijing University of Chemical Technology, P.O. Box 98, Beijing 100029, China

**Email: huizhang67@gst21.com, zhanghui@mail.buct.edu.cn*
Fax: +8610-6442 5385
Tel.: +8610-6442 5872

Preparation of $Au_{25}Capt_{18}$ NCs

The water-soluble, captopril-capped Au_{25} NCs were prepared by a size-focusing synthetic methodology according to a previous report by Jin *et al.*.[1] Typically, 8.23 mL of 10 mg/mL $HAuCl_4·4H_2O$ methanol solution was added into a 25 mL flask containing 1.77 mL of methanol under vigorously magnetic stirring at 25 °C. Then, 126.8 mg of TOABr (0.23 mmol) was added to the solution, and the solution color changed from yellow to deep red. After 20 min, captopril solution (1 mmol, dissolved in 5 mL of methanol) was rapidly injected into above mixture under vigorous stirring. The solution became white. After 30 min, an aqueous solution of $NaBH_4$ (2 mmol, dissolved in 5 mL of ice-cold water) was added rapidly to the mixture under vigorous stirring and the solution immediately turned brown-blackish (photos shown in Figure S1). The reaction was allowed to proceed for 8 h and the reaction mixture was centrifuged (5000 rpm, 20 min) to remove unreacted, insoluble Au(I):SR intermediate complexes. The supernatant was collected and the solvent was removed by rotary evaporation (30 °C, 20 min) followed by adding ethanol (20 mL) and standing overnight to obtain a brown-blackish precipitate, which was dried in vacuum at 30 °C giving a raw product. Then, the raw product was extracted with minimum amount of methanol several times followed by adding ethanol (30 mL) and centrifuging (3000 rpm) for 10 min to obtain a purified brown-black precipitate, which was dried at 30 °C in vacuum overnight giving a purified brown-black product $Au_{25}Capt_{18}$ NCs.

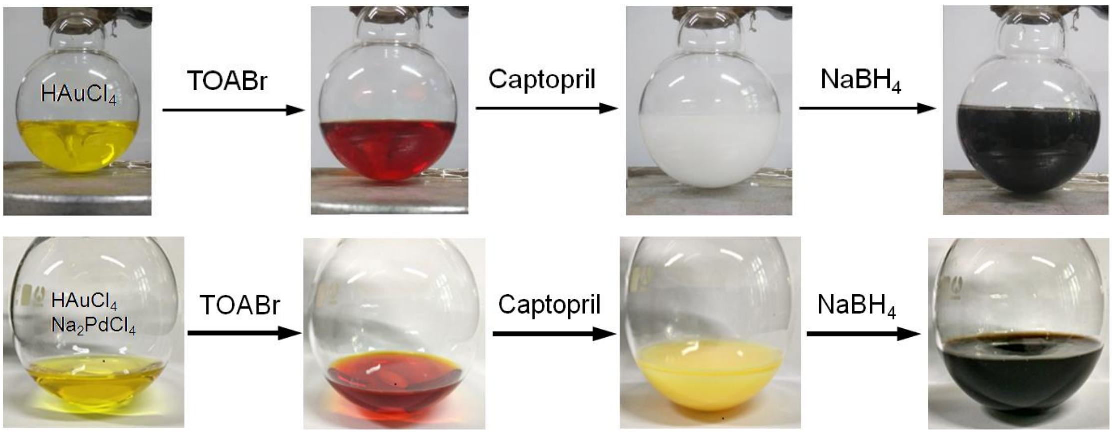

Figure S1. The color changes during the preparation of $Au_{25}Capt_{18}$ (upper) and AuPd NCs (bottom).

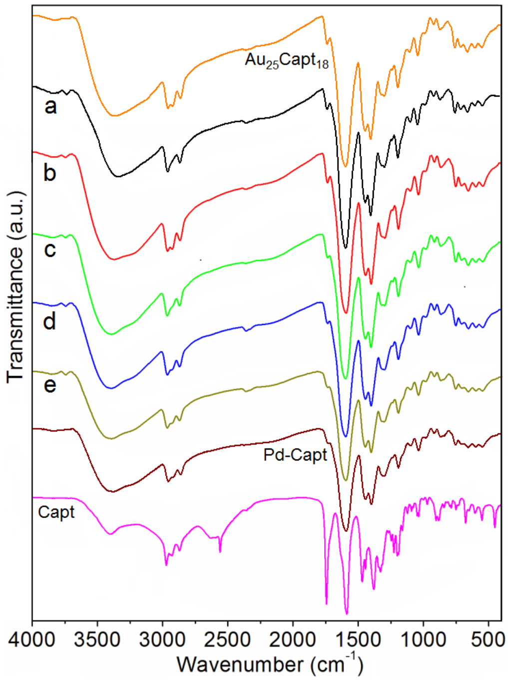

Figure S2. The FTIR spectra of $Au_{96}Pd_4$-Capt (a), $Au_{91}Pd_9$-Capt (b), $Au_{87}Pd_{13}$-Capt (c), $Au_{69}Pd_{31}$-Capt (d),and $Au_{61}Pd_{39}$-Capt (e) compared with $Au_{25}Capt_{18}$, Pd-Capt and Capt.

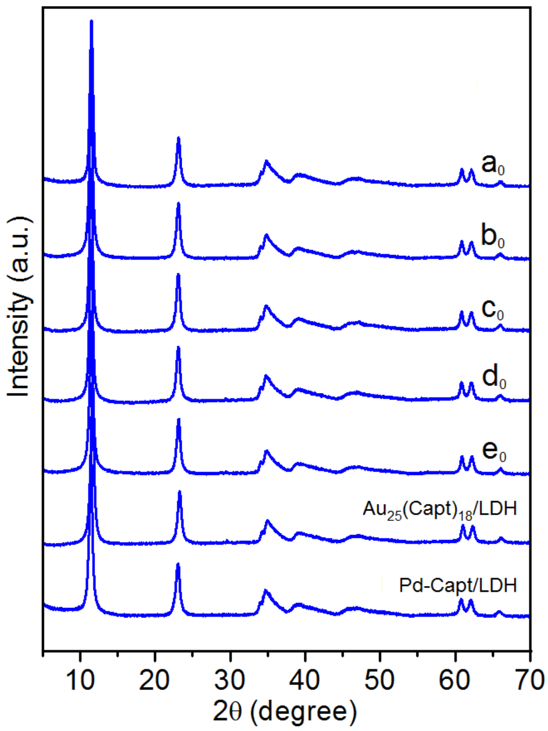

Figure S3. XRD patterns of the catalyst precursors $Au_{96}Pd_4$-Capt/LDH (a_0), $Au_{91}Pd_9$-Capt/LDH (b_0), $Au_{87}Pd_{13}$-Capt/LDH (c_0), $Au_{69}Pd_{31}$-Capt/LDH (d_0), and $Au_{61}Pd_{39}$-Capt/LDH (e_0) compared with $Au_{25}(Capt)_{18}$/LDH and Pd-Capt/LDH.

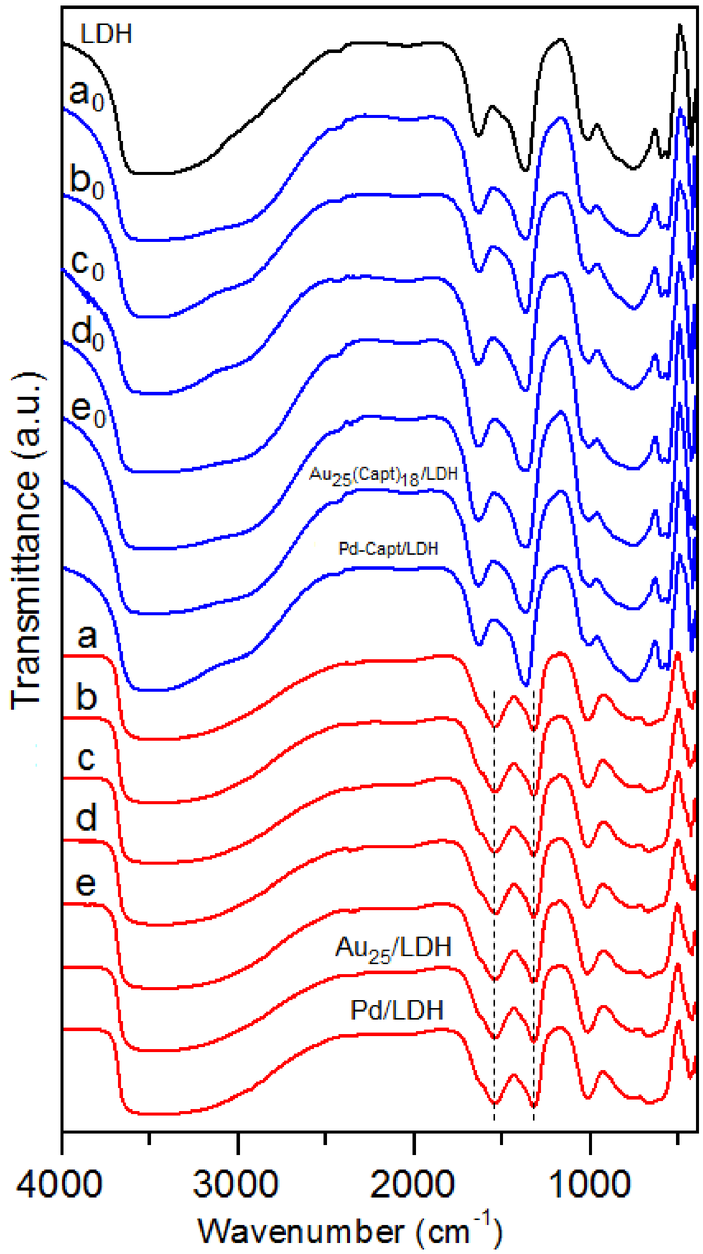

Figure S4. FTIR spectra of $Au_{96}Pd_4$/LDH (a), $Au_{91}Pd_9$/LDH (b), $Au_{87}Pd_{13}$/LDH (c), $Au_{69}Pd_{31}$/LDH (d), and $Au_{61}Pd_{39}$/LDH (e) compared with Au_{25}/LDH, Pd/LDH, corresponding precursors (a_0-e_0), $Au_{25}(Capt)_{18}$/LDH, Pd-Capt/LDH and LDH support.

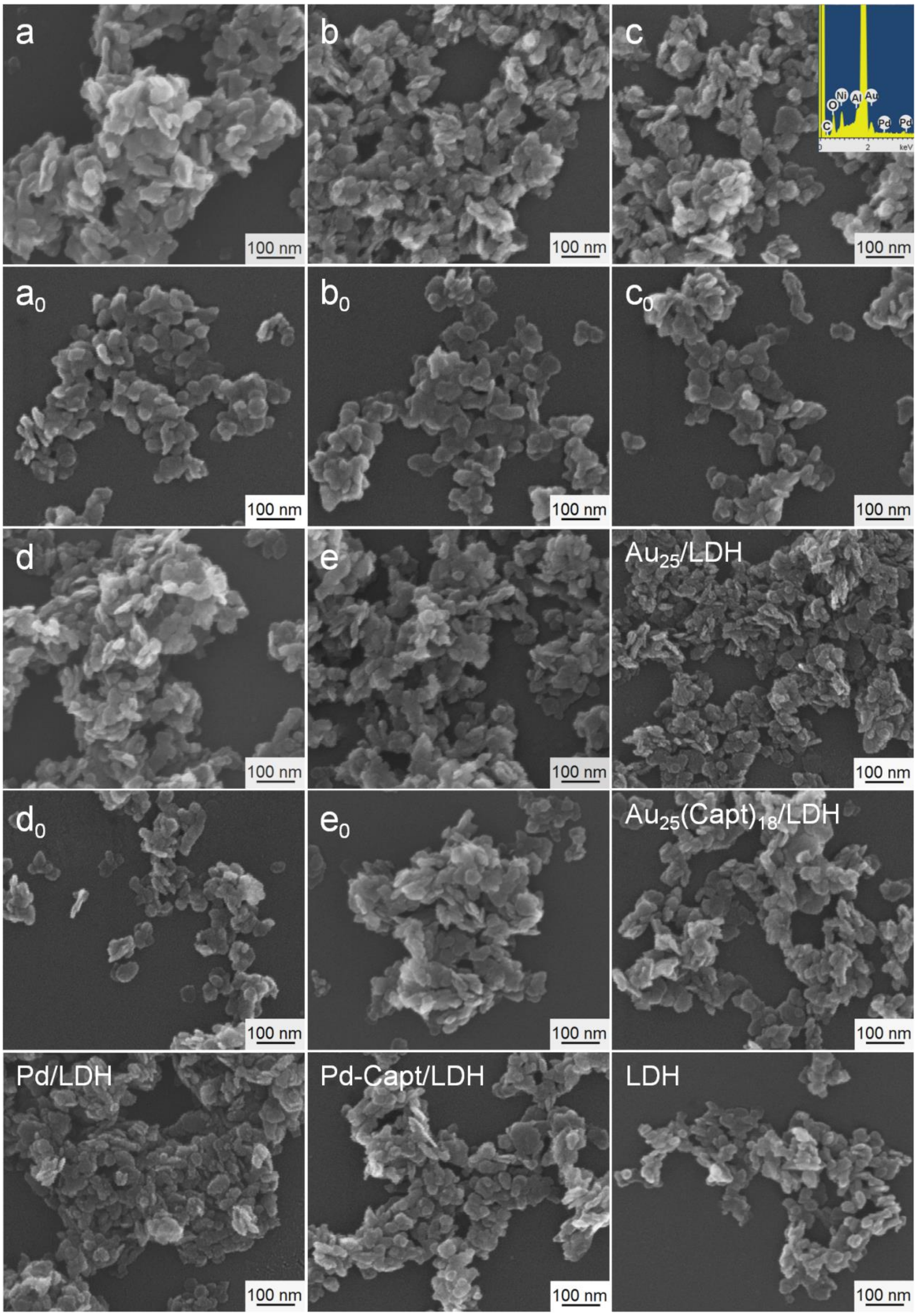

Figure S5. SEM images of $Au_{96}Pd_4$/LDH (a), $Au_{91}Pd_9$/LDH (b), $Au_{87}Pd_{13}$/LDH (c), $Au_{69}Pd_{31}$/LDH (d), and $Au_{61}Pd_{39}$/LDH (e) compared with Au_{25}/LDH, Pd/LDH, corresponding precursors (a_0-e_0), $Au_{25}(Capt)_{18}$/LDH, Pd-Capt/LDH and LDH support.

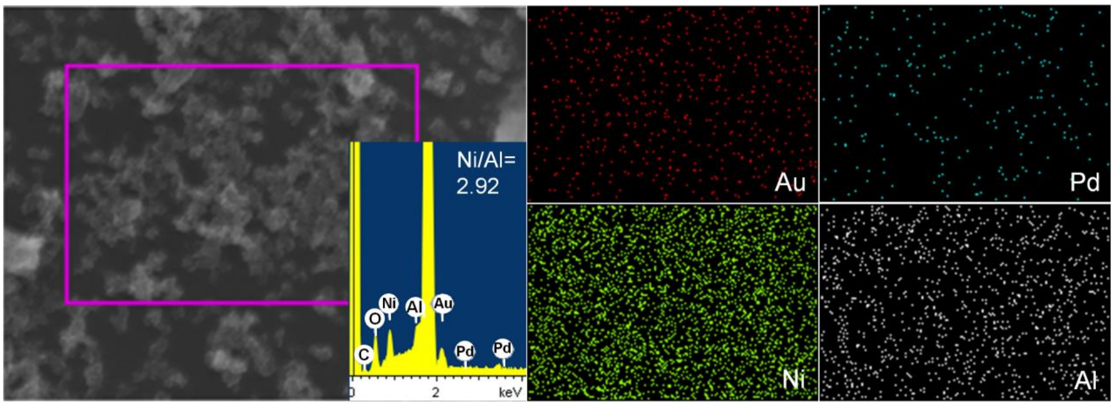

Figure S6. SEM, EDS and metal element mapping images of typical $Au_{87}Pd_{13}$/LDH.

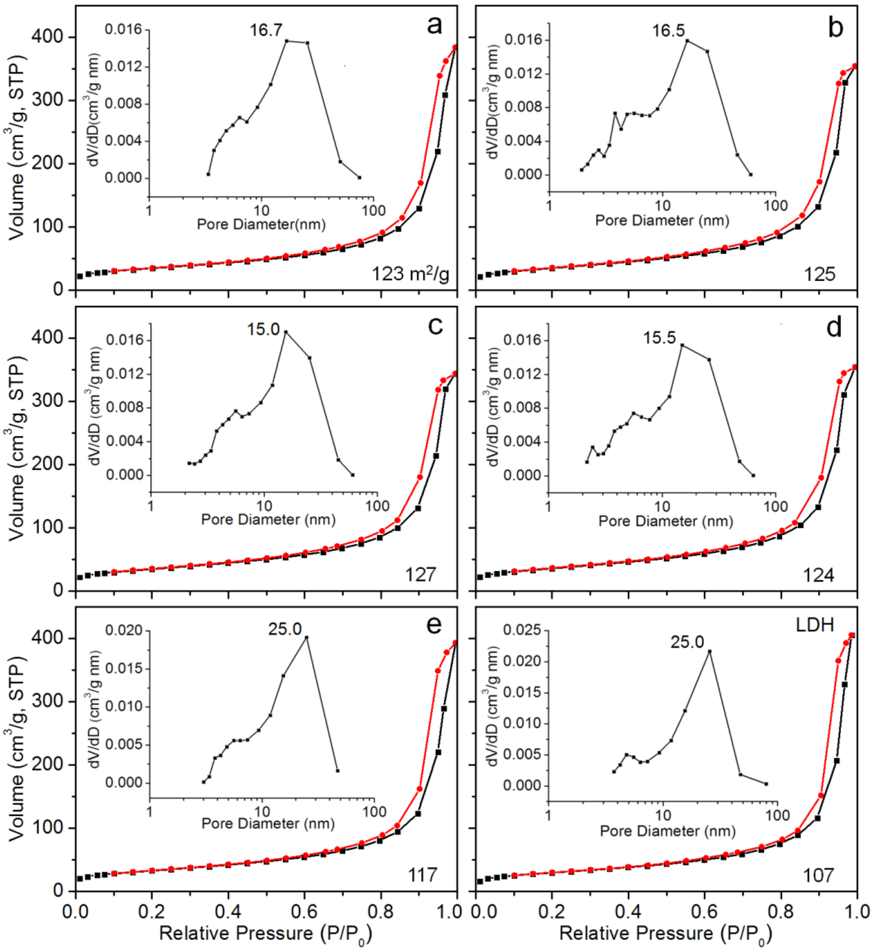

Figure S7. N_2 adsorption-desorption isotherms and pore size distribution curves of $Au_{96}Pd_4$/LDH (a), $Au_{91}Pd_9$/LDH (b), $Au_{87}Pd_{13}$/LDH (c), $Au_{69}Pd_{31}$/LDH (d) and $Au_{61}Pd_{39}$/LDH (e) compared with LDH support.

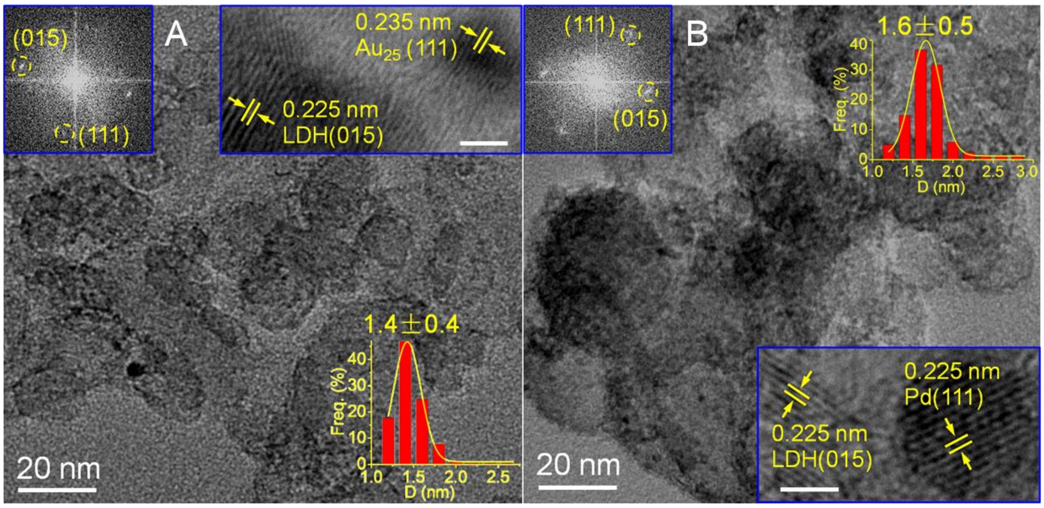

Figure S8. HRTEM images of monometallic Au_{25}/LDH (A) and Pd/LDH (B) (insets: FFT, histogram of particle size distribution and the high-magnification HRTEM (scale bar: 1 nm)).

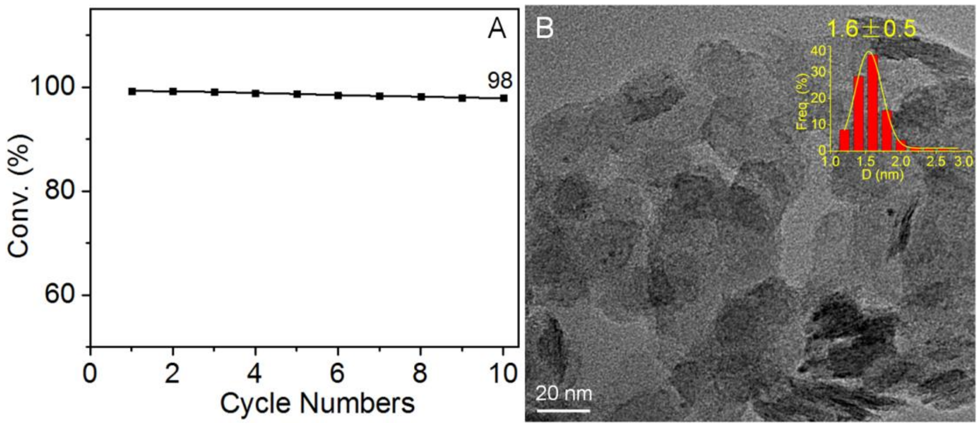

Figure S9. Recycling tests (A) over the $Au_{87}Pd_{13}$/LDH and HRTEM image (B) of the recovered $Au_{87}Pd_{13}$/LDH. Reaction conditions: 1-Phenylethanol (10 mmol), catalyst $Au_{87}Pd_{13}$/LDH (Au: 0.015 mol%), toluene (10 mL), O_2 (20 mL/min), 1 h.

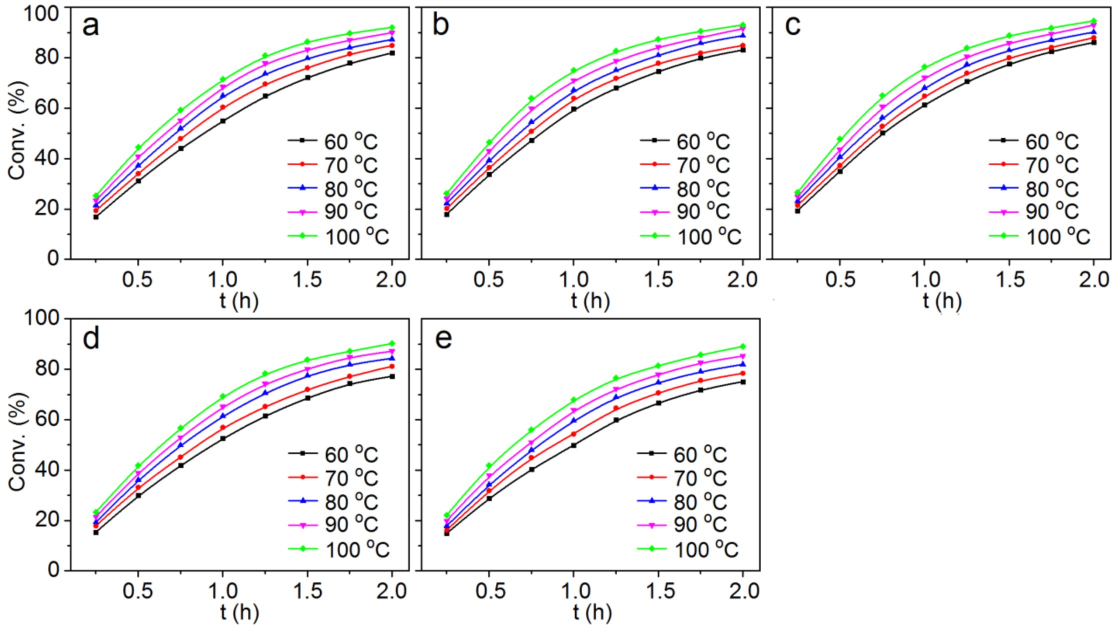

Figure S10. Conversion versus time plots for the oxidation of 1-phenylethanol over the series of catalysts Au_xPd_y/LDH (x/y = 96/4 (a), 91/9 (b), 87/13 (c), 69/31 (d) and 61/39 (e)) at varied reaction temperatures.

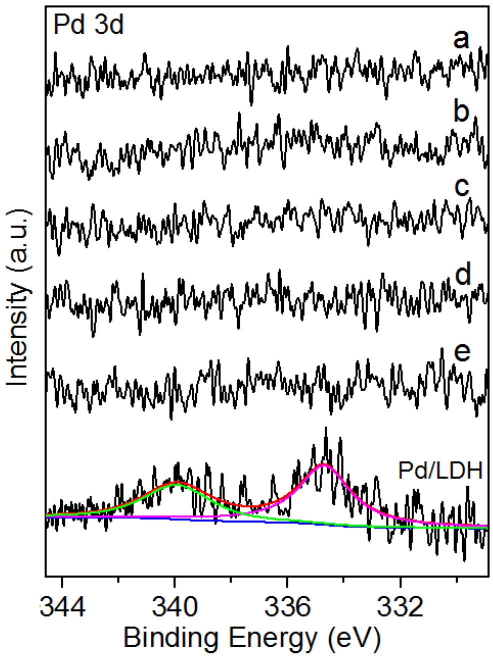

Figure S11. Pd 3d XPS spectra of $Au_{96}Pd_4$/LDH (a), $Au_{91}Pd_9$/LDH (b), $Au_{87}Pd_{13}$/LDH (c), $Au_{69}Pd_{31}$/LDH (d), and $Au_{61}Pd_{39}$/LDH (e) compared with Pd/LDH.

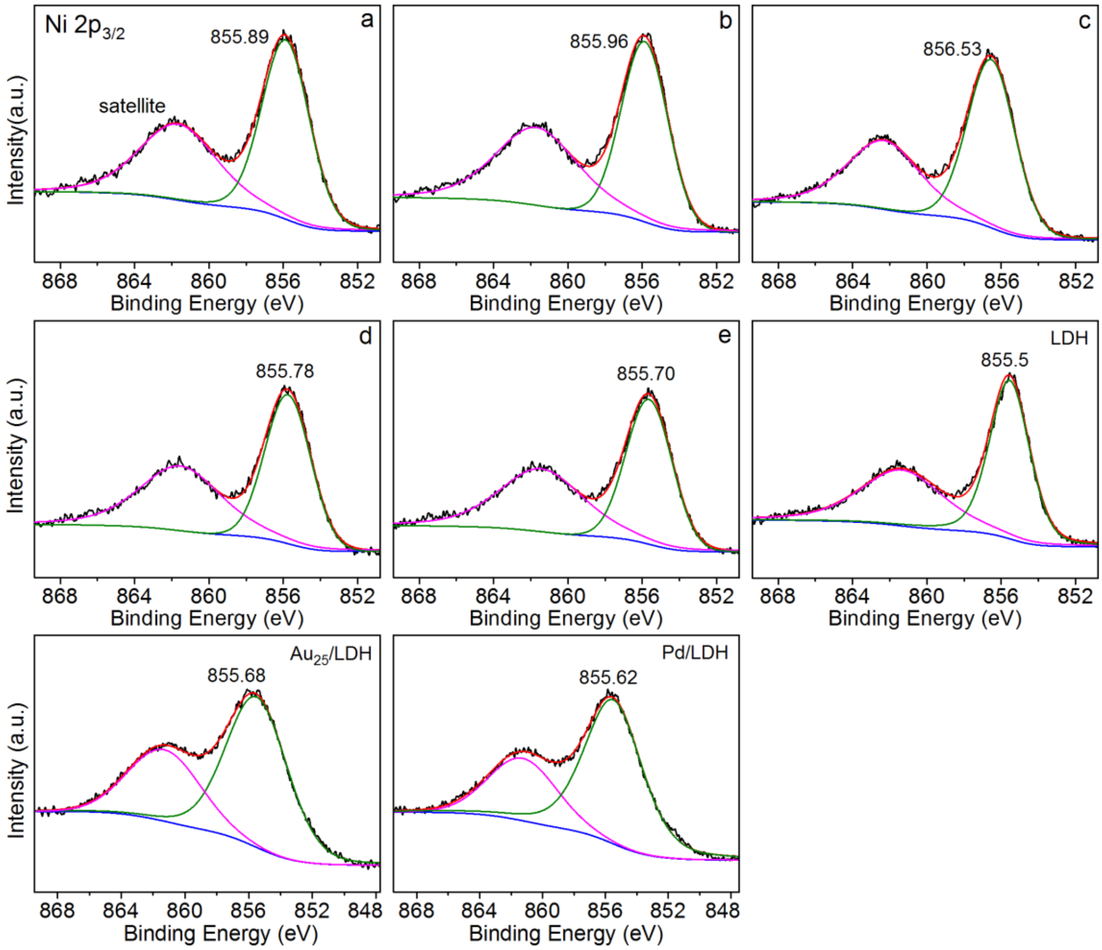

Figure S12. Ni 2p XPS spectra of $Au_{96}Pd_4$/LDH (a), $Au_{91}Pd_9$/LDH (b), $Au_{87}Pd_{13}$/LDH (c), $Au_{69}Pd_{31}$/LDH (d), and $Au_{61}Pd_{39}$/LDH (e) compared with Au_{25}/LDH, Pd/LDH and LDH support.

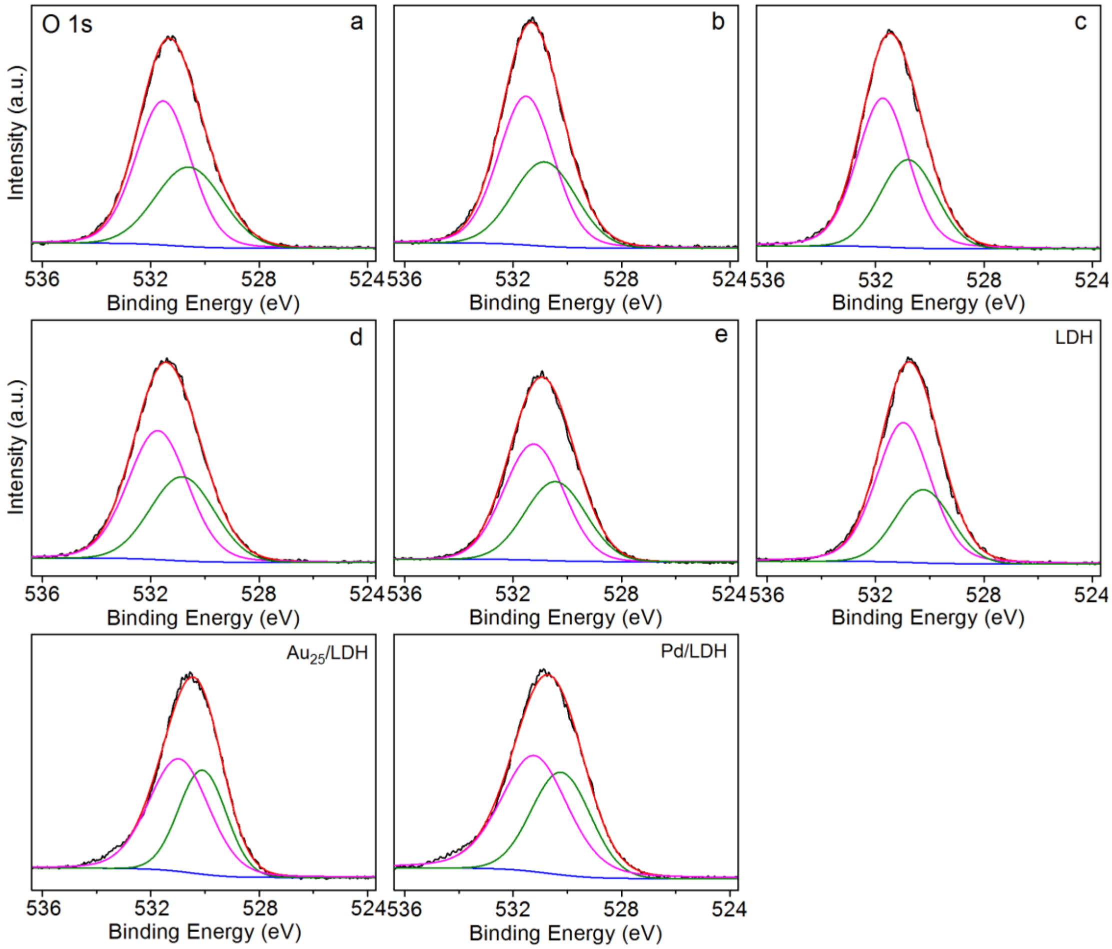

Figure S13. O 1s XPS spectra of $Au_{96}Pd_4$/LDH (a), $Au_{91}Pd_9$/LDH (b), $Au_{87}Pd_{13}$/LDH (c), $Au_{69}Pd_{31}$/LDH (d), and $Au_{61}Pd_{39}$/LDH (e) compared with Au_{25}/LDH, Pd/LDH and LDH support.

Table S1. ICP data of the Au_xPd_y/LDH catalysts compared with the corresponding Au_xPd_y-Capt NCs.

Samples	Au (wt.%)	Pd (wt.%)	Au (at.%)	Pd (at.%)	Au/Pd (mol/mol)[a]
Au_{25}/LDH	0.1982	-	100	0	-
$Au_{96}Pd_4$/LDH	0.1918	0.0043	96.01	3.99	96/4
$Au_{91}Pd_9$/LDH	0.1834	0.0096	91.17	8.83	91/9
$Au_{87}Pd_{13}$/LDH	0.1824	0.0146	87.09	12.91	87/13
$Au_{69}Pd_{31}$LDH	0.1586	0.0384	69.04	30.96	69/31
$Au_{61}Pd_{39}$/LDH	0.1502	0.0521	60.92	39.08	61/39
Pd/LDH	-	0.1922	0	100	-
Clusters	Au (μmol/ml)	Pd (μmol/ml)	Au (at.%)	Pd (at.%)	Au/Pd (mol/mol)[a,b]
$Au_{25}(Capt)_{18}$	0.7376	0	100	-	-
$Au_{96}Pd_4$-Capt/LDH	0.6608	0.0276	95.99	4.01	96/4 (24/1)
$Au_{91}Pd_9$-Capt/LDH	0.4994	0.0506	90.80	9.20	91/9 (23/2)
$Au_{87}Pd_{13}$-Capt /LDH	0.6474	0.0976	86.90	13.10	87/13 (22/3)
$Au_{69}Pd_{31}$-Capt LDH	0.5512	0.2484	68.94	31.06	69/31 (20/5)
$Au_{61}Pd_{39}$-Capt /LDH	0.5947	0.3809	60.96	39.04	61/39 (18/7)
Pd-Capt	0	1.288	0	100	-

[a] Au/Pd ratios based on molar percentages of Au or Pd with respect to total metal (Au + Pd).

[b] Data in brackets refer to theoretical Au/Pd molar ratios.

Table S2. XRD parameters of the series of Au_xPd_y/LDH catalysts compared with corresponding Au_xPd_y-Capt/LDH precursors and LDH support.

Samples	d_{003}(nm)	d_{110}(nm)	c(nm)[a]	a(nm)[a]	D_{003}(nm)[b]	D_{110} (nm)[b]
Au_{25}/LDH	0.679	0.1504	2.037	0.3008	8.918	21.01
$Au_{96}Pd_4$/LDH	0.682	0.1506	2.046	0.3012	8.717	20.88
$Au_{91}Pd_9$/LDH	0.690	0.1508	2.070	0.3016	8.614	20.96
$Au_{87}Pd_{13}$/LDH	0.693	0.1512	2.079	0.3024	8.559	21.09
$Au_{69}Pd_{31}$/LDH	0.683	0.1513	2.049	0.3026	8.748	20.92
$Au_{61}Pd_{39}$/LDH	0.688	0.1510	2.064	0.3020	8.760	20.89
Pd/LDH	0.685	0.1511	2.055	0.3022	8.945	20.91
$Au_{25}Capt_{18}$/LDH	0.762	0.1520	2.286	0.3040	16.12	22.90
$Au_{96}Pd_4$-Capt/LDH	0.762	0.1522	2.286	0.3044	16.10	22.87
$Au_{91}Pd_9$-Capt/LDH	0.762	0.1522	2.286	0.3044	15.95	22.74
$Au_{87}Pd_{13}$-Capt/LDH	0.762	0.1523	2.286	0.3046	15.92	22.68
$Au_{69}Pd_{31}$-Capt/LDH	0.764	0.1520	2.292	0.3040	16.08	22.88
$Au_{61}Pd_{39}$-Capt/LDH	0.764	0.1518	2.292	0.3036	16.12	22.94
Pd-Capt/LDH	0.764	0.1518	2.292	0.3036	16.06	22.84
LDH	0.760	0.1519	2.280	0.3038	16.04	22.95

[a] Based on hexagonal crystal system, $a = 2d_{110}$， $c = 3d_{003}$.

[b] Estimated by Scherrer equation $D_{(hkl)} = 0.89\lambda/\beta\cos\theta$ (λ is X-ray wavelength (Cu Kα: 0.15418 nm), β is half-height width of the diffraction peak in radian, θ is the Bragg diffraction angle in degree).

Table S3. Reaction rate constants of the aerobic oxidation of 1-phenylethanol over the series of catalysts Au_xPd_y/LDH. [a]

Catalysts	k (h^{-1}) [b]					E_a [c] (kJ/mol)
	60 ºC	70 ºC	80 ºC	90 ºC	100 ºC	
$Au_{96}Pd_4$/LDH	0.8481 (0.9973)	0.9912 (0.9964)	1.137 (0.9944)	1.312 (0.9917)	1.524 (0.9879)	15.0 (0.9985)
$Au_{91}Pd_9$/LDH	0.9276 (0.9961)	1.060 (0.9945)	1.209 (0.9927)	1.385 (0.9903)	1.603 (0.9842)	14.0 (0.9963)
$Au_{87}Pd_{13}$/LDH	1.027 (0.9941)	1.191 (0.9930)	1.332 (0.9919)	1.498 (0.9903)	1.712 (0.9876)	12.9 (0.9974)
$Au_{69}Pd_{31}$/LDH	0.760 (0.9945)	0.903 (0.9912)	1.043 (0.9871)	1.197 (0.9854)	1.417 (0.9829)	15.8 (0.9973)
$Au_{61}Pd_{39}$/LDH	0.7245 (0.9965)	0.8789 (0.9943)	1.017 (0.9916)	1.170 (0.9896)	1.388 (0.9864)	16.4 (0.9971)

[a] Reaction conditions: 1-phenylethanol (5 mmol), catalyst (Au: 0.01 mol%), toluene (5 mL), O_2 (20 mL/min), 1 h.

[b] The data in parentheses represent the fitting determination coefficient R^2.

[c] According to Arrhenius equation: k = Aexp(-E_a/RT) (E_a is the apparent activation energy, kJ/mol, k is the reaction rate constant, h^{-1}, A is the pre-exponential factor, h^{-1}, R is the molar gas constant, 8.314 $J \cdot mol^{-1} \cdot K^{-1}$, and T is the absolute temperature, K).

Table S4. XPS data of the series of Au_xPd_y/LDH catalysts compared with the monometallic Au_{25}/LDH, Pd/LDH and LDH support.

Samples	Au $4f_{7/2}$ (eV)	ΔBE (eV)[a]	Pd $3d_{5/2}$ (eV)	Ni $2p_{3/2}$ (eV)	O 1s (eV) (−OH)	O 1s (eV) (O^{2-})
$Au_{96}Pd_4$/LDH	83.10	0.34	n.d.	855.89	531.54 (61.44%)	530.59 (38.56%)
$Au_{91}Pd_9$/LDH	82.97	0.47	n.d.	855.96	531.52 (62.37%)	530.84 (37.63%)
$Au_{87}Pd_{13}$/LDH	82.86	0.58	n.d.	856.53	531.73 (63.29%)	530.79 (36.71%)
$Au_{69}Pd_{31}$/LDH	83.20	0.24	n.d.	855.78	531.74 (60.64%)	530.83 (39.36%)
$Au_{61}Pd_{39}$/LDH	83.29	0.15	n.d.	855.70	531.24 (59.86%)	530.43 (40.14%)
Au_{25}/LDH	83.44	-	-	855.68	531.52 (59.42%)	530.18 (40.58%)
Pd/LDH	-	-	334.71	855.62	531.34 (59.36%)	530.32 (40.64%)
LDH	-	-	-	855.50	530.97 (67.25%)	530.23 (32.75%)

[a] Binding energy shift of Au $4f_{7/2}$ of the Au_xPd_y/LDH catalysts compared with the Au_{25}/LDH.

References

1. Kumar, S.; Jin, R. C. Water-Soluble $Au_{25}(Capt)_{18}$ Nanoclusters: Synthesis, Thermal Stability, and Optical Properties. *Nanoscale* **2012**, *4*, 4222–4227.